Modelling and Trajectory Tracking Control of A 2-DOF Vision Based Inverted Pendulum

Haoping Wang, Christian Vasseur, Vladan Koncar[**], Afzal Chamroo* and Nicolaï Christov

LAGIS - CNRS FRE 3303, Université des Sciences et Technologies de Lille,
UFR IEEA, 59655 Villeneuve d'Ascq Cedex, France
e-mail: (haoping.wang, christian.vasseur, nicolai.christov)@univ-lille1.fr

[**]*GEMTEX, Ecole Nationale Supérieure des Arts et Industries Textiles,*
9 rue de l'Ermitage, 59056 Roubaix, France
e-mail: vladan.koncar@ensait.fr

**LAII, Université de Poitiers, 40, avenue du recteur Pineau, 86022 Poitiers*
e-mail: afzal.chamroo@univ-poitiers.fr

Abstract: *This paper presents a new modelling and trajectory tracking control system of a 2-DOF inverted pendulum using a contactless feedback with a low cost CCD camera. The proposed modelling method transforms the 2-DOF problem into a 1-DOF one by choosing a new balancing plane for the pendulum at each camera sampling instant. For a given plane, two feedback loops are considered. The first one, which is an observation loop, processes the delayed and sampled angle information delivered by the artificial vision system so as to set up a stable linear model of the pendulum and to estimate its continuous state by means of a specific observer called Piecewise Continuous Observer. The second loop, which is a stabilization loop, realizes a Lyapunov function based control to stabilize the cart-pendulum system. Simulation results illustrate the performances of the proposed approach.*

Keywords: 2-DOF inverted pendulum, visual servoing control, piecewise continuous observer.

1. INTRODUCTION

The inverted pendulum system is a perfect benchmark for a wide range of nonlinear control design methods because of its inherent instability and highly non-linear dynamics. The most considered inverted pendulums are: single, double or triple inverted pendulum on a cart [1-8], a rotational single-arm or two-link pendulum [8-9] and an inverted pendulum on an x-y robot [10-13]. In almost all cases, controllers use continuous accurate sensors which are in physical contact with the pendulum.

However, in numerous applications it is impossible to put sensors in direct contact with the controlled object. Vision systems are a means to avoid this physical constraint. Moreover, from an economical point of view it may be interesting to develop robust control methods that do not require expensive high accuracy sensors.

In this paper we consider the design of an inverted pendulum control system using a low cost CCD camera as contactless pendulum sensor. The problem is that this type of sensors are less accurate and often deliver sampled and delayed signals due to their digital nature and computation-transfer time (image processing) respectively.

Using visual feedback to control a robot is commonly termed as visual servoing [14-16]. For example visual (image based) features such as points, lines and regions can be used to enable the alignment of a manipulator/gripping mechanism with an object. Hence, vision is a part of a control system providing feedback. However, traditionally visual sensing and manipulation are combined in an open-loop configuration, 'looking' and 'moving' [9], or just for visualizations and animations [17]. Recently, visual supervision has been gradually combined in the closed control loop particularly for cart-inverted pendulum control such as in [18-19]. Unfortunately there is no real successful application reported on controlling the pendulum and the cart position by visual servoing till now. Only a fuzzy-logic based controller was reported in [20], but just for controlling the pendulum. The PID+Q controller has been applied to antisway control of crane lifter modeled by the structure of an inverted pendulum [21]. Unfortunately, there is no research work related to an inverted pendulum on an x-y robot using visual feedback has been reported.

Analyzing difficulties of previous vision based research works related to inverted pendulum control; it seemed that the camera signal has not been sufficiently exploited. Therefore, our efforts have been focused on the development of the accurate observer using the theory of Piecewise Continuous Systems (PCS) [22] to compensate the delayed, imprecise sampled data of the vision system. The improved signal is generated in continuous time.

The research results presented here are an extension and development of the previous works [22-28] especially relative to the use of the PCS in order to design a PCO that compensates the time delay and the sampling effects introduced by the visual feedback.

In this article, the control scheme implemented via a cascade combination method is inspired by the work of K. Guemghar

et al. [29]. The control method based on a PCO and linearization and stabilization control applied to control the pendulum angle form the inner loop. In parallel, a Lyapunov based control for the unstable non-minimum-phase internal system (cart) with slower dynamics comparing to the pendulum dynamics constitutes the outer loop. Simulation results are given to illustrate the performances of the proposed control system.

2. EXPERIMENTAL PLATFORM

The vision based control platform of the 3D inverted pendulum, presented in Fig. 1, contains the following parts:

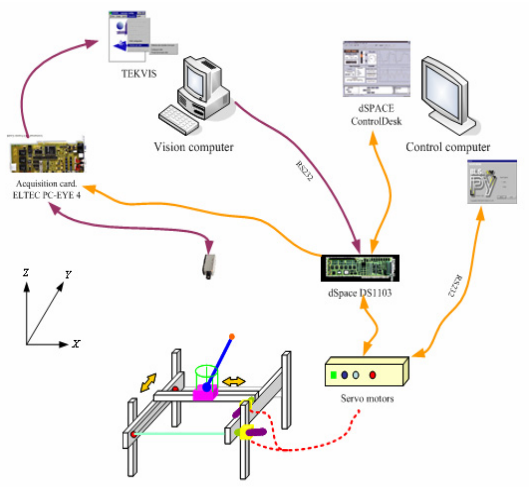

Fig. 1. Experimental 2-DOF inverted pendulum

2.1. The Mechanical X-Y table (Fig. 1)

The system is composed of an X-Y aluminum chassis and a plastic inverted pendulum mounted on the mobile cart. Between the pendulum and the cart, a circular shock absorber preventing the pendulum from completely falling to horizontal position is installed. It allows the pendulum to have a maximum angle ±30° (can be changed) with respect to the vertical position. Axes are actuated by AC servo motors via notched belt.

2.2. The controller

The controller is implemented using a dSpace DS1103 card on a control computer. The ControlDesk module integrated with Matlab/Simulink, enables the modeling, the supervision and the development of direct control methods for the real system using control card variables and parameters. The control signals are sent to power amplifiers via ± 10 V DAC.

2.3. The actuators

This part of the system is composed of two servo motors (SANYO DENKI PY2A015A3-A3), whose configurations can be modified and parameterized via the RS-232 serial communication by the PY software in the control computer. AC motors P50B050020DXS00M, driven by a dSpace computer input/output card via a power amplifier, are actually mounted on each axis of the X-Y table. The amplifier is supplied with 240 V. The AC motors deliver a nominal couple of 3.0 Nm with a power of 200 W. The platform provides the cart *x, y* position through encoders.

2.4. Vision system

Instead of using hi-tech digital cameras capable of higher sampling rates, higher spatial resolution and improved signal/noise ratio, a low cost IR CCD (Jai M50 IR) camera is used with a sampling rate of 25 frames/sec and a low resolution of 640 × 480 pixels in non-interlaced mode. The measurements of the camera are available at a sampling rate of T = 40 ms (acquisition-processing-transferring time). In order to simplify the data sensing, an infrared LED has been added on the upper tip of pendulum.

The vision computer is equipped with an image acquisition card (ELTEC PC-EYE 4). Image processing is realized by software called TEKVIS that detects the inverted pendulum's upper tip (*x,y*) coordinates and transmits them to the control computer via the RS-232 serial communication. In order to synchronize the camera with the controller, the camera is triggered by an external periodical pulse signal, generated via the dSpace card with a sampling period equal the acquisition-processing-transferring time.

As soon as the control computer receives the pendulum coordinates, a four step "TSAI" calibration method [30] is carried out. It supports not only the real inverted pendulum top position but also the compensation of the deformations caused by the camera lenses. Moreover, the difference in the height of the pendulum upper tip plays an important role in the projective imaging geometry of the camera. Hence, two points with a same coordinate in x-y plane but in different height project to two different points in the image, affecting the sensing results and accuracy.

3. MODELLING THE VISION BASED 2-DOF INVERTED PENDULUM

3.1. Classical linearization modelling method

In [5-6], [13], [26], the authors propose an approximately decoupled modeling method for a 2-DOF inverted with the constraint of working in a small angle inclination $\theta \le 10°$. The obtained pendulum model has the form

$$\begin{aligned}
&(M_x + m)\ddot{x} + ml\ddot{\alpha}\cos\alpha - ml\dot{\alpha}^2\sin\alpha + c_{M_x}\dot{x} = u_x \\
&J\ddot{\alpha} - mgl\sin\alpha = -ml\ddot{x}\cos\alpha \\
&(M_y + m)\ddot{y} + ml\ddot{\beta}\cos\beta - ml\dot{\beta}^2\sin\beta + c_{M_y}\dot{y} = u_y \\
&J\ddot{\beta} - mgl\sin\beta = -ml\ddot{y}\cos\beta
\end{aligned} \tag{1}$$

where M_x and M_y are the platform mass with respect to x-axis and y-axis, m is the mass of the pendulum, l is the length from the pendulum center of gravity to the pivot, c_{M_x} and c_{M_y} are the friction coefficients in x and y directions, $J=(ml^2)/3$ is the pendulum momentum of inertia, and α, β are the projection angles with respect to *xOz* and *yOz* plans.

As compared to this method, we propose here a different modeling approach without any restriction. Its main idea consists in choosing an optimal plane in view of transforming a 2-DOF inverted pendulum problem in a 1-DOF problem.

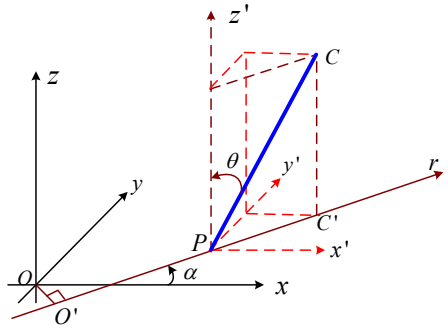

Fig. 2. Projection on the r-z and x-y-z planes

3.2. *Proposed modelling method*

Initially, we consider the *Px'y'z'* reference parallel to the *Oxyz* reference of the cart-pendulum system, with point *P* being the pivot of the pendulum. At any time, the inverted pendulum can be projected onto two orthogonal planes: r-z' (including the entire inverted pendulum) and x-y plane (parallel to two directions of the X-Y table), as illustrated in Fig.2. According to the main modeling idea, the r-z' plane has been chosen as the optimal one to balance the pendulum. Thus, the 2-DOF problem is reduced to a 1-DOF one.

By referring to the methods proposed in [1], [3], the 2-DOF inverted pendulum can be modeled as

$$\ddot{\theta} + 2\zeta\omega_n\dot{\theta} - \omega_n{}^2 \sin\theta = -K\cos\theta\ddot{r} \tag{2}$$

where θ is the angle of the pendulum with z-axis in the r-z' plane, $\omega_n = \sqrt{mgl/(J+ml^2)}$ is the natural frequency, $\zeta = B_r/[2\omega_n(J+ml^2)]$ is the damping ratio, $K = ml/(J+ml^2)$ is the gain, r is the cart position on r-axis, B_r is the viscous damping constant between the pendulum and the cart, g the gravitational acceleration. The origin of r-axis is *O'* which is the orthogonal projection of *O* on r-axis.

Moreover, by considering the projection of the pendulum on the x-y plane, as shown in Fig. 3,

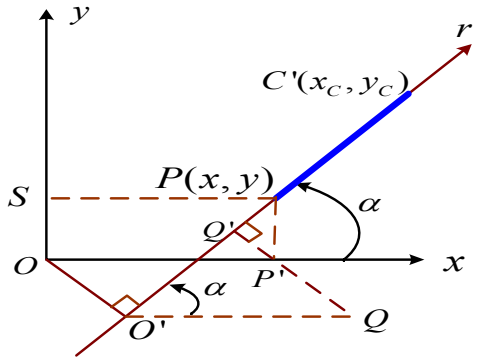

Fig. 3. Projection on x-y plane

we can find the geometrical relationship between *x, y* and *r*:

$$r = x\cos\alpha + y\sin\alpha \tag{3}$$

with α the angle between r and x axes and calculated by (6).

On x-axis, the motor-cart model which considers the motor terminal voltage u_x as its input and the motor horizontal displacement x as its output, can be modeled as

$$\ddot{x} = (-\dot{x} + k_x u_x)/\tau_x \tag{4}$$

where k_x is the overall gain of the motor-cart on x-axis and τ_x is the time constant of the motor-cart on x-axis.

In the same way, the motor-cart on y-axis is modeled as

$$\ddot{y} = (-\dot{y} + k_y u_y)/\tau_y . \tag{5}$$

3.3. *Pendulum Angles Computation (α and θ)*

According the structure of our platform, the only accessible information are the coordinates (x_C, y_C) of the pendulum upper tip projection on the x-y plane via the vision system and the pendulum pivot coordinates (x,y) via x and y encoders.

In these conditions, according to Fig. 2 and Fig. 3, the α and θ angles can be computed as

$$\begin{aligned} \alpha &= \tan^{-1}\left[(y_C - y)/(x_C - x)\right], \\ \theta &= \sin^{-1}\left\{\left[(x_c - x)\cos\alpha + (y_c - y)\sin\alpha\right]/2l\right\}. \end{aligned} \tag{6}$$

In our case, only sampled and delayed measurements are available (see Fig. 4):

$$(x_C((k-1)t_e), y_C((k-1)t_e)) = (x_{C,k-1}, y_{C,k-1}) \tag{7}$$

where t_e is the camera sampling cycle. For our vision system, t_e=40 ms. From (6) and (7), α_{k-1} and θ_{k-1} are computed.

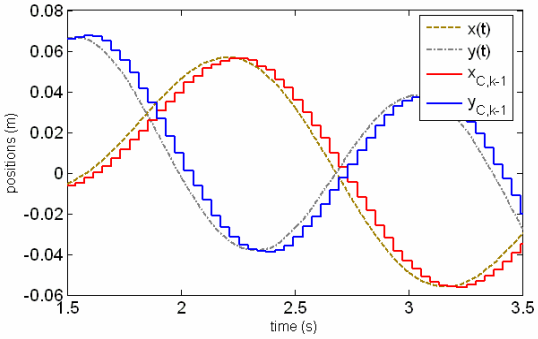

Fig. 4. Measurements of Fixed vertical pendulum

4. VISUAL SERVOING CONTROL

The main control architecture for the 2-DOF pendulum is presented in Fig. 5. The hybrid feedback generates the continuous cart coordinates (x,y) and the delayed and sampled pendulum angular position θ_{k-1}. The control principle is that at each sampling instant an optimal balancing

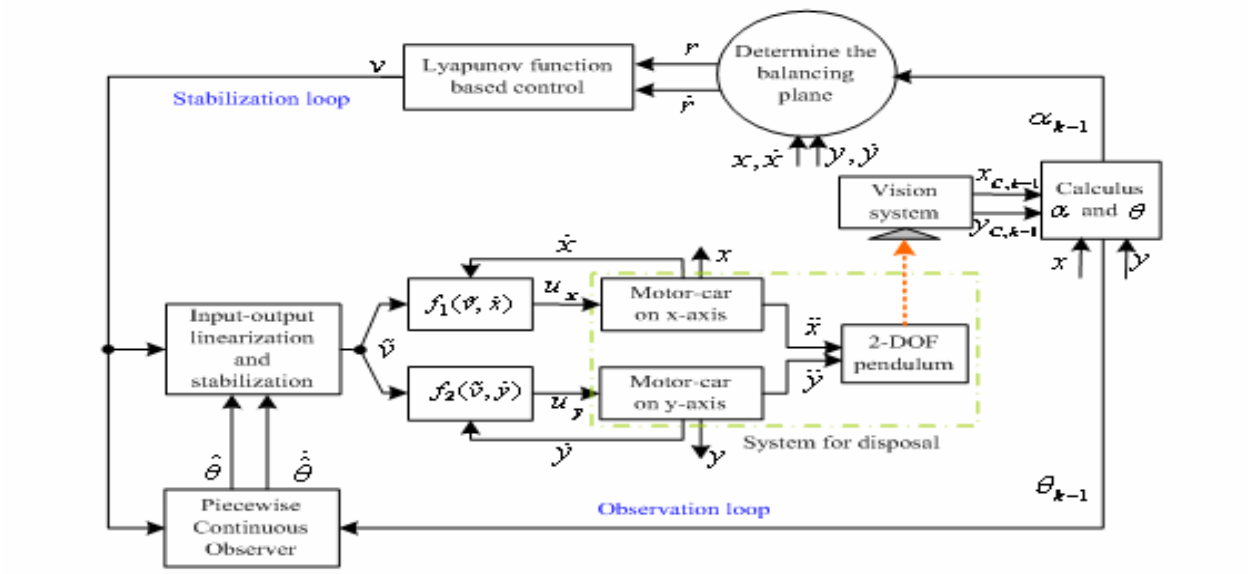

Fig. 5. Trajectory tracking architecture for 2-DOF inverted pendulum

plane r-z' is selected by using α_{k-1}. Then, in this balancing plane, a control system is built consisting of two loops. The first one (inner loop) realizes a linearization and the stabilization control of the pendulum based on the innovative Piecewise Continuous Observer (PCO) coupled with a linearization module. The second one (the outer loop) realizes a Lyapunov based control for the unstable internal system having slower dynamics than that of the pendulum.

The aim is to find two controls u_x and u_y by introducing an intermediate pendulum reference angle θ_{ref} which ensures the global stability of the 2-DOF cart-pendulum system.

4.1. Linearization and stabilization of the 2-DOF Inverted Pendulum using piecewise continuous observer

Under the assumption that the inverted pendulum angular position θ and velocity $\dot{\theta}$ are precisely estimated via the PCO, the 1-DOF inverted pendulum dynamic equations in (1) lead to

$$\ddot{r} = \tilde{v}\,, \tag{8}$$

$$\ddot{\theta} + 2\zeta\omega_n\dot{\theta} - \omega_n{}^2 \sin\theta = -K\cos\theta\tilde{v}. \tag{9}$$

In order to stabilize the pendulum, a stable dynamics can be imposed by introducing a new control v, a new gain K_2, a new natural frequency Ω_n and a new damping ratio Z defined as

$$-2\zeta\omega_n\dot{\theta} + \omega_n{}^2\sin\theta - K\cos\theta\tilde{v} = -2Z\Omega_n\dot{\theta} - \Omega_n^2\theta + K_2 v. \tag{10}$$

From (10) the relation between $\tilde{v}$ and v is

$$\tilde{v} = [-2(\zeta\omega_n - Z\Omega_n)\dot{\theta} + \Omega_n^2\theta + \omega_n{}^2\sin\theta - K_2 v]/K\cos\theta \tag{11}$$

with $|\theta| < \pi/2$. After the transformation, one has

$$\ddot{r} = [-2(\zeta\omega_n - Z\Omega_n)\dot{\theta} + \Omega_n^2\theta + \omega_n{}^2\sin\theta - K_2 v]/K\cos\theta, \tag{12}$$

$$\ddot{\theta} + 2Z\Omega_n\dot{\theta} + \Omega_n^2\theta = K_2 v. \tag{13}$$

Thus, from (13), the linearized pendulum state equation is

$$\dot{\Theta}(t) = A\Theta(t) + Bv(t) \tag{14}$$

with $A = \begin{bmatrix} 0 & 1 \\ -\Omega_n^2 & -2Z\Omega_n \end{bmatrix}$, $B = \begin{bmatrix} 0 \\ K_2 \end{bmatrix}$ and $\Theta(t) = \begin{bmatrix} \theta(t) \\ \dot{\theta}(t) \end{bmatrix}$.

Consider now the estimation of the continuous position θ and velocity $\dot{\theta}$ using a PCO. This observer consists of a Reduced-Order Discrete Luenberger Observer (RODLO) and two Piecewise Continuous Systems (PCS) as shown in Fig. 6.

A PCS $\Sigma(\{kt_e\}, A, B, C)$ is characterized by a continuous input $\varphi(t)$, an input $\psi(t)$ sampled at discrete instants kt_e, state, input and output matrices A, B, C, a state vector $x(t)$ and an output vector $y(t)$ [22]. PCS dynamics is described as

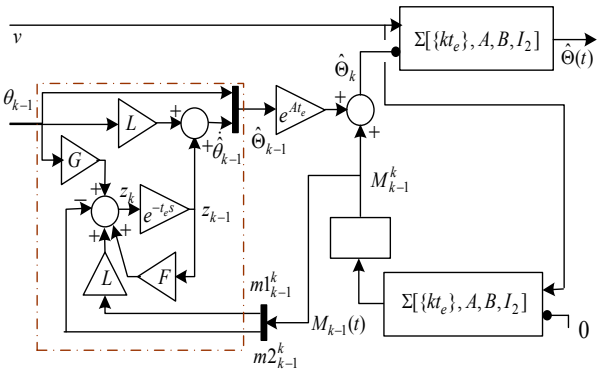

Fig. 6. Piecewise Continuous Observer

$$x_k(t) = \exp(A(t-kt_e))\psi(kt_e) + \int_{kt_e}^{t} \exp A(t-\tau)B\varphi(\tau)d\tau, \tag{15}$$

$$y_k(t) = Cx_k(t),\ \forall t \in [kt_e, (k+1)t_e[\ .$$

In PCO A and B are chosen as in (14) and $C=I_2$.

According to Fig. 6, the PCO is designed in the following way.

First step: PCS I

For PCS I, with $\varphi(t)=v(t)$ and $\psi(t)=0$, one has

$$M_{k-1}(t)=\int_{(k-1)t_e}^{t}\exp A(t-\tau)Bv(\tau)d\tau. \quad (16)$$

By sampling (ZOH) at each kt_e, one obtains

$$M_{k-1}^{k}=\int_{(k-1)t_e}^{kt_e}\exp A(kt_e-\tau)Bv(\tau)d\tau=\begin{bmatrix} m1_{k-1}^{k} \\ m2_{k-1}^{k}\end{bmatrix}.$$

Second step:RODLO

Θ_{k-1} is estimated by the RODLO

$$z_k=Fz_{k-1}+G\theta_{k-1}+(m2_{k-1}^{k}-Lm1_{k-1}^{k}), \quad (17a)$$

$$z_{k-1}=\dot{\hat{\theta}}_{k-1}-L\theta_{k-1}, \quad (17b)$$

where

$$F=(f_{22}-Lf_{12}),$$
$$G=(f_{22}-Lf_{12})L+(f_{21}-Lf_{11}),$$
$$L=(f_{22}/f_{12})\in R$$

and $\exp(At_e)=\begin{bmatrix} f_{11} & f_{12} \\ f_{21} & f_{22}\end{bmatrix}$.

The value of L is chosen to maximize the observer convergence speed.

Estimating $\dot{\theta}_{k-1}$ by $\dot{\hat{\theta}}_{k-1}=z_{k-1}+L\theta_{k-1}$, one gets $\hat{\Theta}_{k-1}$, then $\hat{\Theta}_k$, by integration of (14) on the time interval $[(k-1)t_e, kt_e[$, one has

$$\hat{\Theta}_k=\exp(At_e)\hat{\Theta}_{k-1}+M_{k-1}^{k}. \quad (18)$$

Third step: PCS II

Using PCS II with $\varphi(t)=v(t)$ and $\psi(t)=\hat{\Theta}_k$, one has

$$\hat{\Theta}(t)=\exp(At)\hat{\Theta}_k+\int_{kt_e}^{t}\exp A(t-\tau)Bv(\tau)d\tau. \quad (19)$$

4.2. Lyapunov Function Based Cascade Control

The main idea of the control scheme is to introduce an angular reference θ_{ref} as an intermediate for the pendulum angular position in the aim of finding the two controls (u_x, u_y).

In the first step, using the quasi-steady state assumption [29], [31] for (12) and (13), i.e. $\ddot{\theta}=\dot{\theta}=0$, it is possible to define a trajectory reference $\theta=\theta_{ref}$. Thus the corresponding equations become

$$\ddot{r}=\tilde{v}=[\omega_n{}^2\tan(\theta_{ref})]/K, \quad (20)$$

$$v=(\Omega_n^2\theta_{ref})/K_2. \quad (21)$$

In the second step, based on this internal 2-DOF pendulum system, we define a Lyapunov candidate function

$$V(r,\dot{r})=(\chi r^2+\delta\dot{r}^2)/2, \text{ with } \chi,\delta>0. \quad (22)$$

In order to ensure

$$\dot{V}(r,\dot{r})=\dot{r}(\chi r+\delta\ddot{r})=\dot{r}(\chi r+\delta\tilde{v})<0, \quad (23)$$

a particular function stabilizing the internal dynamics is chosen as

$$(\chi r+\delta\tilde{v})=-\mu[1-e^{-(\chi r^2+\delta\dot{r}^2)/2}]\dot{r}, \quad \mu>0. \quad (24)$$

Therefore, one has

$$\tilde{v}=-[\chi r+\mu(1-e^{-(\chi r^2+\delta\dot{r}^2)/2})\dot{r}]/\delta. \quad (25)$$

By replacing (25) in (20), θ_{ref} can be computed as

$$\theta_{ref}(r,\dot{r})=\tan^{-1}\left\{-K[\chi r+\mu(1-e^{-(\chi r^2+\delta\dot{r}^2)/2})\dot{r}]/(\delta\omega_n{}^2)\right\} \quad (26)$$

From (22)-(24) it follows that the control (25) stabilizes the cart position and velocity ($r=\dot{r}=0$). Consequently, according to (26), it appears that the stabilization of the cart leads to $\theta_{ref}(0,0)=0$ and thus to $v=0$. According to (14), $v=0$ makes possible to obtain $\theta=\dot{\theta}=0$. The introduction of $\theta_{ref}(r,\dot{r})$ in (20) and (21) ensures the stability of the cart-pendulum system.

Then, from (20) and (26), we obtain the control

$$v=\Omega_n^2\tan^{-1}\left\{-K[\chi r+\mu(1-e^{-(\chi r^2+\delta\dot{r}^2)/2})\dot{r}]/(\delta\omega_n{}^2)\right\}/K_2. \quad (24)$$

The last step is to find the relations between the control $\tilde{v}$ and the two control signals u_x and u_y (see Fig. 5). Considering (3), (4) and (5) with local input/output injection for each motor, we can obtain $k_x=k_y=k$ and $\tau_x=\tau_y=\tau$. In these conditions, the balancing of the pendulum in the r-z' plane is ensured by imposing the following additional condition for the cart accelerations:

$$\ddot{y}/\ddot{x}=\tan\alpha.$$

Finally, u_x and u_y are defined as

$$u_x=f_1(\tilde{v},\dot{x})=(\dot{x}+\cos\alpha\tau\tilde{v})/k, \quad (27)$$

$$u_y=f_2(\tilde{v},\dot{y})=(\dot{y}+\sin\alpha\tau\tilde{v})/k. \quad (28)$$

5. NUMERICAL RESULTS

In the experimental platform shown in Fig. 7, the pendulum mass is 560 g and its length is 31.5 cm, the viscous friction

between the pendulum and the cart on the x-y robot is $B_r = 0.001$. Therefore, according to the previous modeling considerations, the inverted pendulum is characterized by

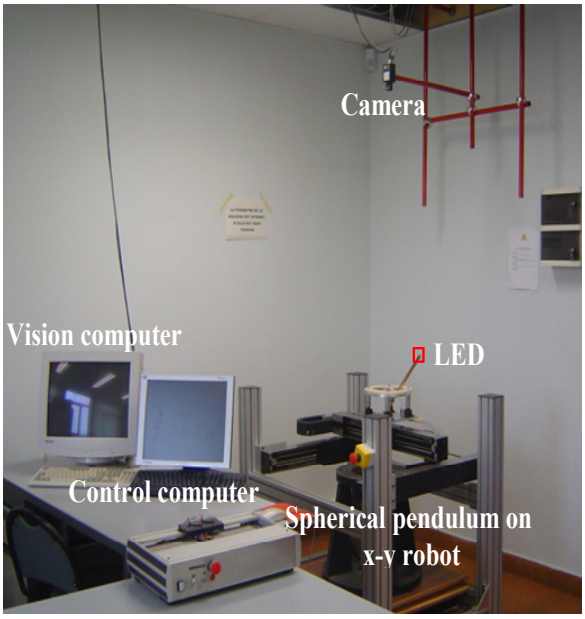

Fig. 7. Experimental platform

$\zeta = 0.0039$ and $\omega_n = 6.781$ rad/s.

For the application of local feedback, the parameters of the motor-cart on each axis are set as $k = 2.92$ and $\tau = 0.008$. For the controller part, we choose $K_2 = \omega_n^2$, $\xi = 1.2$, $\Omega_n = \omega_n$, $\chi = 1$, $\delta = 2$ and $\mu = 0.5$ by taking into account the system performance and stability.

Because of the dSpace card limited capacity, the proposed method at this moment is only implemented for x-axis (illustrative videos are available on http://www-lagis.univ-lille1.fr/~wang/Research_eng.html). That is why the performances of the proposed 2 DOF pendulum control system are analyzied by simulation.

For initial conditions $\alpha_0 = \pi/3$ rad, $\theta_0 = \pi/6$ rad, $x_0 = 1$ m and $y_0 = 0.2$ m, Fig. 8 shows: (a) balancing plane projected in x-y plane, (b) *x*, *y* and *r* displacements, (c) the errors of pendulum angular positions ($\theta(t) - \theta_{k-1}$, $\theta(t) - \hat{\theta}(t)$), (d) the error of pendulum angular velocity ($\dot{\theta}(t) - \hat{\dot{\theta}}(t)$) and (e) the corresponding control signals (u_x, u_y).

Fig. 8a, 8b and 8c show that the proposed two loops control leads to the stabilization of the 2-DOF cart-pendulum system, the cart being stabilized around *O'* (projection of *O* on the balancing plane and origin of r axis).

Note that the quasi-steady state assumption doesn't bring any restriction: no permanent oscillation appears, neither on the displacement of the cart, nor on the pendulum. The simulation results demonstrate that $\theta_{ref}(r, \dot{r})$ ensures the stability of the system.

Moreover, from Fig. 8c and 8d, it can be seen that the PCO gives very good estimations of the pendulum angular position $\theta(t)$ and velocity $\dot{\theta}(t)$ after a very short transition.

As in all mechanical systems, uncertainty and variation of the parameters are inevitable. In order to study the robustness of the proposed control, we add simultaneously a parameter variation of $B_r \sin 2\pi t$ in the parameter B_r and measurement errors of $0.01\sin 2\pi t$ on θ_{k-1} and $0.01\sin 2\pi t$ on α_{k-1}. The corresponding simulation results are shown in Fig. 9. It can be seen that despite of these perturbations, the spherical pendulum system remains stable. The PCO still gives satisfactory estimations.

6. CONCLUSION

This article presents the modelling and visual servoing control of 2-DOF spherical inverted pendulum by using a hybrid feedback afforded by a low cost camera and two encoders. At each camera sampling instant, the control determines a balancing plane which transforms the 2-DOF problem into a 1-DOF. Then in this plane, the proposed control consists of two feedback loops. The first one processes the delayed and sampled angle information delivered by the artificial vision system so as to set up a stable linear model of the pendulum and to estimate its continuous state by means of PCO. The second loop makes use of a Lyapunov function based control in order to stabilise the cart-pendulum system. The numerical results demonstrate the effectiveness of the proposed control approach.

REFERENCES

Armando A.R., Richard P., Oguzhan C. and Thanate D., - "Description of a modelling, simulation, animation, and real-tile control (MoSART) environment for a class of electromechanical systems", *IEEE Trans. on Education*, 48 (3), **359-374**, 2005.

Bugeja M., - "Non-linear swing-up and stabilizing control of an inverted pendulum system", *EUROCON*, 2003.

Chamroo A., Vasseur C. and Wang H.P., - "Plant control using digital sensors that introduce a delayed and sampled output", *11th ELMA World Congress*, 1, **119-124**, 2005.

Chen L. and Smith R., - "Closed-loop model validation for an inverted pendulum experiment via a linear matrix inequality approach", *Proc. Of the 36th CDC*, **2565-2566**, 1997.

Chesi G., - "Optimal Object Configurations to Minimize the Positioning Error in Visual Servoing", *IEEE Transactions on Roboticis*, Vol. 26 (3), **384-386**, June 2010.

Cho H. and Jung S., - "Balancing and Position Tracking Control of an Inverted Pendulum on an X-Y Plane Using Decentralized Neural Networks", *Proc. of 2003*

IEEE/ASME Inter. Conf. on Advanced Intelligent Mechatronics, **1210-1215**, 2003

Cho H. and Jung S., - "Neural Network Position Tracking Control of an Inverted Pendulum by an X-Y Table Robot", *Proc. of the 2003 IEEB/RSJ Int. Conf. on Intelligent Robots and Systems*, **181-186**, 2003.

Deley D. W., - "Controlling an inverted pendulum: example of a digital feedback control system", *http://members.cox.net/srice1/pendulum/index.htm.*

Espinoza-Quesada E.S. and Ramos-Velasco L.E., - "Vision based control of an underactuated system using a reduced observer", *Electronics, Robotics and Automotive Mechanics Conference,* 1*,* **9-14***,* 2006.

Fierro R., Lewis F.L. and Lowe A., - "Hybrid control for a class of underactuated mechanical systems", *IEEE Trans. on Systems, Man, and Cybernetics-Part A: Systems and Humans*, 29 (6), **649-654**, 1999.

Guemghar K., Srinivasan B., Mullhaupt Ph. and Bonvin D., - "Analysis of cascade structure with predictive control and feedback linearization", *IEE Control Theory & Applications*, 152 (3), **317-324**, 2005

Heikkila J. and Silven O., "A four-step camera calibration procedure with implicit image correction", *IEEE Computer Society Conference on Computer Vision and Pattern Recognition*, Jun 1997.

Hutchinson S., Hager G.D. and Corke P.I., - "A tutorial on visual servo control", *IEEE Trans. on Robotics and Automation*, 12 (5), **651-670**, 1996.

Isidori A., - "nonlinear control systems", Springer, 3rd edition, 1994.

Jung S. and Cho H.T., - "Decoupled neural network reference compensation technique for a PD controlled two degrees-of-freedom inverted pendulum", *Int. J. of Control, Automation and Systems*, 2 (1), **92-99**, 2004.

Koncar V. and Vasseur C., - "Control of linear systems using piecewise continuous systems", *IEE Control Theory & Applications*, 150(6), **565-576**, 2003.

Linderoth M., Robertsson A., Astrom K. and Johansson R., - "Object Tracking with Measurements from Single or Multiple Cameras", *IEEE Inter. Conf. Robotics and Automation,* Anchorage, Alaska, USA 2010.

Lozano R., Fantoni I. and Block D. J., - "Stabilization of the inverted pendulum around its homoclinic orbit", *Systems & Control Letters*, 40, **194-204**, 2000.

Magana M.E. and Holzapfel F., - "Fuzzy-logic control of an inverted pendulum with vision feedback", *IEEE Trans. On Education*, 41 (2), **165-170**, 1998.

Matsuo T., Yoshino R., Suemitsu H. and Nakano K., - "Nominal performance recovery by PID+Q controller and its application to antisway control of crane lifter with visual feedback", *IEEE Trans. on Control System Technology*, 12 (1), **156-166**, 2004.

Ohsumi A. and Izumikawa T., - "Nonlinear control of swing-up and stabilization of an inverted pendulum", *Proc. Of the 34th CDC*, **3873-3880**, 1995.

Olfati-Saber R., - "Fixed point controllers and stabilization of the cart-pole system and the rotating pendulum," *Proc. Of the 38th CDC*, **1174-1181**, 1999.

Sanchez J., Dormido S., Pastor R. and Morilla F., - "A Java/Matlab-based environment for remote control system laboratories: illustrated with an inverted pendulum," *IEEE Trans. on Education*, 47 (3), **321-329**, 2004

Wang H. P., Vasseur C. and Koncar V., - "Piecewise continuous systems used in trajectory tracking of a vision based x-y robot", Novel Algorithms and Techniques In Telecommunications, Automation and Industrial Electronics, Springer Netherlands, ISBN 978-1-4020-8736-3, 2008

Wang H. P., Vasseur C., Chamroo A. and Koncar V., - "Hybrid control for vision based Cart-inverted Pendulum system", *ACC'08, American Control Conference*, **3845 – 3850**, 2008

Wang H. P., Vasseur C., Chamroo A. and Koncar V., - "Sampled tracking for delayed systems using piecewise functioning controller", *4th IEEE conf. on Computational Engineering in Systems Applications*, 2, 2006.

Wang H. P., Vasseur C., Chamroo A. and Koncar V., - "Stabilization of a 2-DOF inverted pendulum by a low cost visual feedback", *ACC'08, American Control Conference*, **3851 – 3856**, 2008

Wang H. P., Vasseur C., Koncar V., Chamroo A. and N. Christov, - "Design and implementation of robust hybrid control of vision based underactuated mechanical nonminimum phase systems", *Studies in Informatics and Control*, Vol. 19 (1), **35-44**, 2010

Wei Q., Dayawansa W.P. and Levine W.S., - "Nonlinear controller for an inverted pendulum having restricted travel", *Automatica*, 31 (6), **841-850**, 1995.

Wenzel L., Vazquez N., Nair D. and Jamal, R., - "Computer vision based inverted pendulum", *Proc. of the 17th IEEE Instrumentation and Measurement Technology Conference*, 3, **1319-1323**, 2000.

Yang R., Kuen Y. and Li Z., - "Stabilization of A 2-DOF Spherical Pendulum on X-Y Table", *Proc. Of the 2000 IEEE International Conference on Control Applications*, **724-729**, 2000.

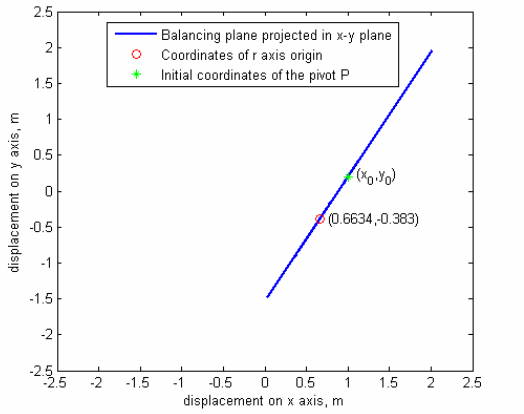

(a) Balancing plane projected in x-y plane

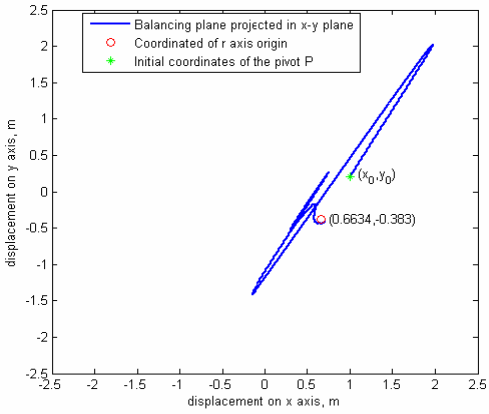

(a) Balancing plane projected in x-y plane

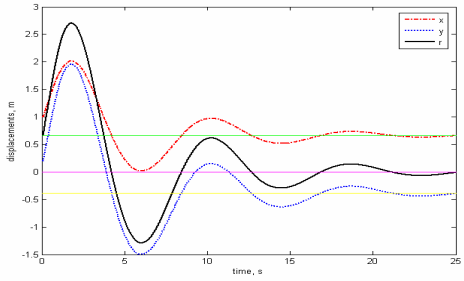

(b) *x, y* and *r* displacements

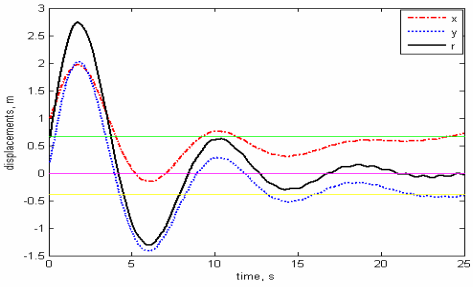

(b) *x, y* and *r* displacements

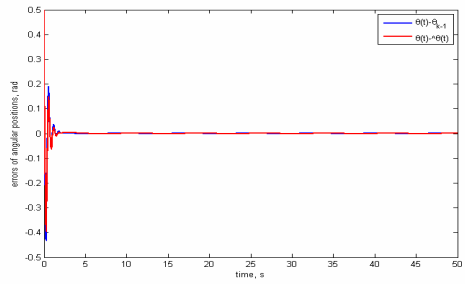

(c) $\theta(t)-\theta_{k-1}$, and $\theta(t)-\hat{\theta}(t)$

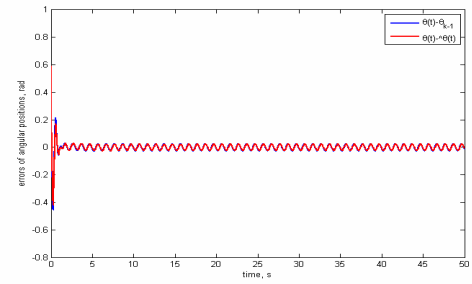

(c) $\theta(t)-\theta_{k-1}$, and $\theta(t)-\hat{\theta}(t)$

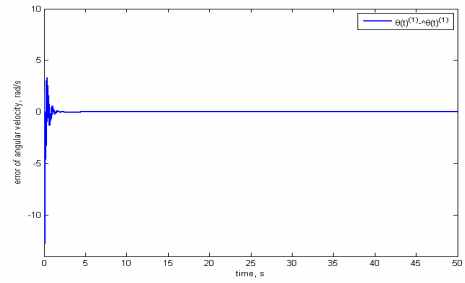

(d) $\dot{\theta}(t)-\dot{\hat{\theta}}(t)$

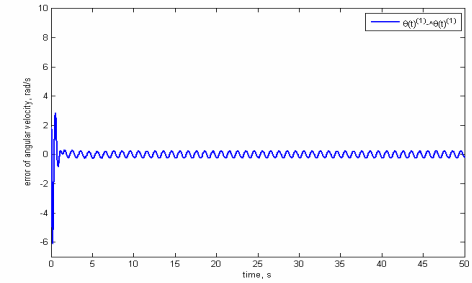

(d) $\dot{\theta}(t)-\dot{\hat{\theta}}(t)$

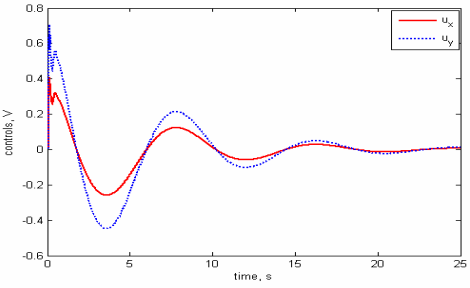

(e) Controls u_x and u_y

Fig. 8. Simulation results without modeling errors

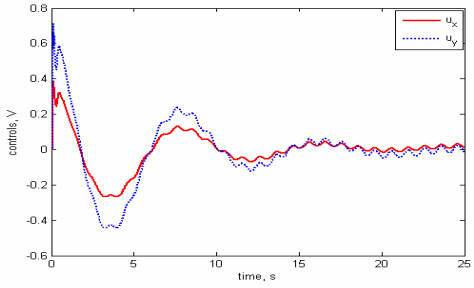

(e) Controls u_x and u_y

Fig. 9. Simulation results with modeling errors